Probing Leptogenesis with the Cosmological Collider

Yanou Cui[1,*] and Zhong-Zhi Xianyu[2,3,†]

[1]*Department of Physics and Astronomy, University of California, Riverside, California 92521, USA*
[2]*Department of Physics, Tsinghua University, Beijing 100084, China*
[3]*Collaborative Innovation Center of Quantum Matter, Beijing 100084, China*

Leptogenesis is generally challenging to directly test due to the very high energy scales involved. In this Letter, we propose a new probe for leptogenesis with cosmological collider physics. With the example of a cosmological Higgs collider, we demonstrate that during inflation leptogenesis models can produce detectable primordial non-Gaussianity with distinctive oscillatory patterns that encode information about the lepton-number violating couplings, the Majorana right-hand neutrino masses, and the *CP* phases, which are essential to leptogenesis.

Introduction.—Leptogenesis is an attractive mechanism explaining the origin of the baryon asymmetry in our universe, and it is closely related to the seesaw mechanism for the origin of neutrino masses [1–6]. In the simplest leptogenesis scenario, a lepton asymmetry is generated from the decay of a heavy right-handed (RH) neutrino N, which is then transferred to a baryon asymmetry via the sphaleron process. Despite the appeals of leptogenesis, it is very challenging to directly test it, as the very high energy scales involved are generally beyond the reach of terrestrial experiments, in contrast to some of the low scale baryogenesis models (e.g., [7–21]). For instance, with hierarchical masses of N_i ($i = 1, 2, 3$), a lower bound exists for the lightest N's mass: $M_1 \gtrsim 10^9$ GeV [22].

In this Letter, we demonstrate that, thanks to the high energies provided by the cosmic inflation, leptogenesis may leave distinct and observable signatures in primordial non-Gaussianity (NG), inspired by the cosmological collider (CC) physics. In particular, the essential Sakharov conditions for leptogenesis such as L-number violation and *CP* violation, as well as the heavy RH neutrino masses, can be probed individually as they impact the CC signals in different ways. Our finding also leads to new types of fermionic CC signatures that are not yet considered in the literature.

CC physics has been recently developed as a method to probe heavy particles during cosmic inflation [23–51]. The energy scale of inflation, characterized by the nearly constant Hubble parameter H, can be up to $O(10^{13})$ GeV in single-field slow-roll models. Different versions of CC

exist. The original version is an inflaton collider: by coupling to the inflaton, heavy particles with masses up to $O(H)$ imprint the n-point ($n \geq 3$) correlators of the curvature perturbation ζ. An alternative version, called the cosmological Higgs collider (CHC) [34], exploited the possibility that an appreciable component of ζ is originated from the quantum fluctuations of the standard model (SM) Higgs field H during inflation, through the modulated reheating process [52–55]. Compared with the original CC, CHC has the advantage of yielding large and detectable NG with less free parameters. With these considerations, along with the fact that the SM Higgs directly participates in leptogenesis via the Yukawa coupling, in this Letter we will focus on signals with the CHC.

Cosmological Higgs collider.—Quantum fluctuation during inflation generates a space dependent vacuum expectation value (VEV) $v \sim H$ for the Higgs field. In the program of CHC, this VEV controls the inflaton decay rate and by doing so imprints its spatial dependence on the fluctuations of the local time of reheating. Consequently, the Higgs fluctuations δh can source at least a fraction of primordial curvature perturbation $\zeta = \zeta_0 + \zeta_h$, where ζ_h is the fluctuation from Higgs modulated reheating and ζ_0 denotes other contributions such as from the inflaton fluctuations. Then we can write $\zeta_h = (2\pi P_\zeta^{1/2}/H)R_h\delta h$ at the linear level, where $R_h = \zeta_h/\zeta$ and $P_\zeta \sim 2 \times 10^{-9}$ is the measured scalar power spectrum. Thus the three-point correlator (bispectrum) of ζ_h is related to the three-point correlator of δh as

$$\langle\zeta_{h,\mathbf{k}_1}\zeta_{h,\mathbf{k}_2}\zeta_{h,\mathbf{k}_3}\rangle = \left(\frac{2\pi P_\zeta^{1/2}R_h}{H}\right)^3 \langle\delta h_{\mathbf{k}_1}\delta h_{\mathbf{k}_2}\delta h_{\mathbf{k}_3}\rangle. \quad (1)$$

In the original proposal [34], the fraction R_h is roughly 10%, but this is model dependent. The upshot is that ζ_h, while being a small fraction of ζ, can contribute to most of
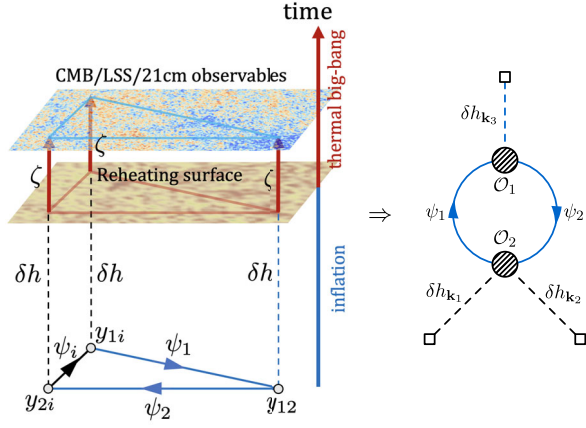
FIG. 1. One-loop process contributing to SM and Majorana RH neutrino signals at the CHC ($i = 1, 2$).

the NG. In this Letter, we treat R_h as a free parameter, $0 < R_h < 1$. Furthermore, the working of CHC requires that the Higgs potential is stabilized and that the Higgs is lighter than H during the inflation. While this might call for new physics beyond SM, we note that the signal considered below only depends on the neutrino properties and is essentially independent of the new physics that stabilized the Higgs potential.

Equation (1) shows that the primordial bispectrum in CHC can reveal information about Higgs interactions during inflation. In particular, particles with masses $m \sim H$ may leave a signal in the bispectrum if they couple to the SM Higgs. In this Letter, we are interested in the signals mediated by neutrinos represented by the one-loop diagram on the left side of Fig. 1 (we will explain the right diagram in the next section).

The signal shows up for squeezed bispectrum where $k_1 \simeq k_2 \gg k_3$ ($k_i \equiv |\mathbf{k}_i|$, $i = 1, 2, 3$), as a characteristic oscillatory function of the momentum ratio $\varrho \equiv k_3/k_1$. It is useful to express the signal in terms of a dimensionless and (nearly) scale-invariant shape function $\mathcal{S}(k_1, k_2, k_3) \equiv (k_1 k_2 k_3)^2/(4\pi^2 P_\zeta)^2 \langle \zeta_{h,\mathbf{k}_1} \zeta_{h,\mathbf{k}_2} \zeta_{h,\mathbf{k}_3} \rangle'$ (' symbol means the momentum-conserving δ function removed) as (see Ref. [50] for more details)

$$\lim_{\varrho \to 0} \mathcal{S}(\varrho) = f_{\mathrm{NL}}^{(\mathrm{signal})} \varrho^\alpha \sin(\omega \log \varrho + \vartheta), \quad (2)$$

where $f_{\mathrm{NL}}^{(\mathrm{signal})}$ is the amplitude of the signal. The dimensionless quantities $(\alpha, \omega, \vartheta)$ measure the scaling behavior, the frequency, and the phase of the oscillatory signal. They are in principle measurable and also calculable for specific processes. It is known that the signal with a Dirac fermion of mass m in a one-loop diagram has $\alpha = 3$ and $\omega = 2m/H$ [34]. A key result of this Letter is that the Majorana mass of the RH neutrino and CP phases innate to the leptogenesis mechanism can generate new patterns in the signal. In particular, the CHC signal with a Majorana neutrino gives

$\alpha = 2$ instead of 3, and the CP phases give rise to more than one value of ω, and the signal would be superpositions of different oscillation patterns.

Leptogenesis, neutrino masses, and CP phases during inflation.—Leptogenesis mechanism meets the Sakharov conditions in the following ways: (1) lepton number violation via the Majorana masses of the RH neutrinos N's; (2) CP violation via the CP phases in the Yukawa couplings through the tree-loop interference in N decay; and (3) out of equilibrium via the decay process [1,56].

A key observation is that, with a Majorana mass term, the mass matrix and the Higgs couplings cannot be simultaneously diagonalized. This results in a new type of Yukawa coupling mixing different mass eigenstates with distinct CHC signals. The following derivations closely follow the standard neutrino seesaw model, with the key difference that $\boldsymbol{H}$'s VEV is typically around the inflationary Hubble scale H, and consequently the neutrino mass and mixing pattern is very different in the inflation and postinflation eras.

One generation suffices to demonstrate how the mixed coupling arises. Consider the usual Type I seesaw with one generation of N and SM lepton doublet $L = (\nu, e^-)^T$. In CHC the Higgs gets a nonzero VEV $v \sim H$ during inflation due to quantum fluctuations. Here, the inflationary Hubble parameter H is required to be higher than electroweak scale for the original CHC mechanism [34] to work. Parametrizing the Higgs as $\boldsymbol{H} = (0, (v + h)/\sqrt{2})^T$ and focusing on neutrinos only, we have

$$\Delta \mathcal{L} = \nu^\dagger i \bar{\sigma}^\mu \partial_\mu \nu + N^\dagger i \bar{\sigma}^\mu \partial_\mu N$$
$$+ \left[m_D \left(1 + \frac{h}{v} \right) \nu N - \frac{1}{2} m_N N N + \mathrm{c.c.} \right], \quad (3)$$

where $m_D \equiv yv/\sqrt{2}$. The $U(2)$ symmetry of the kinetic term allows us to choose m_D and m_N to be real without loss of generality, and also to rotate to mass eigenstates $\psi_\pm$ with mass eigenvalues $m_\pm = \frac{1}{2}(m_N \pm \sqrt{m_N^2 + 4m_D^2})$. In the postinflationary epoch, Higgs resides in its true vacuum such that $m_D \ll m_N$, and thus $m_- \ll m_+$, realizing the seesaw mechanism after electroweak phase transition. But during inflation $m_D \sim m_N \sim H$ is likely, therefore $\psi_\pm$ could have comparable masses.

Although these are mostly familiar results, the important point is that the Higgs coupling matrix cannot be simultaneously diagonalized by the above rotations. Rather, it takes the following form after the rotation:

$$\mathcal{L} \supset \frac{m_D h}{v \sqrt{m_N^2 + 4m_D^2}} [m_D(\psi_-^2 - \psi_+^2) + m_N \psi_- \psi_+], \quad (4)$$

with a nonzero trilinear coupling that mixes $\psi_\pm$ when $m_N \neq 0$. As we will see, this mixed Yukawa coupling in the mass eigenstates can give rise to a unique signal in

three-point function of Higgs, and thus can be viewed as a signature of Majorana neutrino mass.

A realistic leptogenesis model typically involves three generations of RH N's. With nonzero Majorana mass terms, the above result of Yukawa coupling to mixed mass eigenstates still apply, but with the new feature that these couplings generally contain irremovable CP phases. As we will see below, these phases introduce yet another new pattern in the CHC signal.

Cosmological (Higgs) collider signals of leptogenesis.— A key result from the above discussion is that the Yukawa couplings mix different mass eigenstates and carry nonzero complex phases. Now we demonstrate their distinctive physical consequences on the CHC observables.

The central object is the three-point correlator of the Higgs fluctuation, namely the left diagram in Fig. 1. The CHC signal appears when the blue lines carry momenta much smaller than the black lines, i.e., in the squeezed limit. In this configuration it proves advantageous to take an effective field theory limit for the bottom black line in the triangle, which effectively shrinks the line into a point vertex [57], as shown in the right diagram of Fig. 1. Then it is straightforward to use the diagrammatic rule [30] to write down an expression for this process:

$$\langle \delta h_{k_1} \delta h_{k_2} \delta h_{k_3} \rangle' = \sum_{a,b=\pm} ab \int_{-\infty}^{0} d\tau_1 d\tau_2 a^4(\tau_1) a^4(\tau_2)$$
$$\times G_a(k_1, \tau_1) G_a(k_2, \tau_1) G_b(k_3, \tau_2)$$
$$\times \mathcal{I}(k_3; \tau_1, \tau_2), \quad (5)$$

where τ is conformal time, $a = -1/(H\tau)$ is the scale factor, $a, b = \pm$ are Schwinger-Keldysh indices, G_a is the boundary-to-bulk δh propagator and $\mathcal{I}$ is the fermion one-loop integral including couplings:

$$\mathcal{I}(k; \tau_1, \tau_2) = \int d^3 X e^{-ik \cdot X} \langle \mathcal{O}_1(\tau_1, X) \mathcal{O}_2(\tau_2, 0) \rangle. \quad (6)$$

Now we explain the effective operators $\mathcal{O}_{1,2}$. We can write the most general Yukawa coupling mixing a pair of mass eigenstate as

$$\Delta \mathcal{L} = \delta h \mathcal{O}_1, \qquad \mathcal{O}_1 \equiv y_{12} (e^{i\varphi_{12}} \psi_1 \psi_2 + \text{c.c.}), \quad (7)$$

where $\psi_{1,2}$ are Weyl spinors and mass eigenstates with masses $m_{1,2}$. Generally, $m_1 \neq m_2$ ($m_1 = m_2$) with (without) the presence of Majorana mass in the original Lagrangian. We set y_{12} real and positive and isolate the CP phase φ_{12}. $\mathcal{O}_1$ accounts for the upper vertex in the right diagram in Fig. 1. The diagonal case $\mathcal{O}_1 = y_{ii} \psi_i \psi_i + \text{c.c.}$ ($i = 1, 2$) can also contribute to the signal, but this is not mass mixing and the signal would be identical to the case of "Dirac" to be discussed below. When the diagonal case contribution is

present and sizable, the new signal in this Letter can be extracted by dedicated template fitting.

The lower vertex in the right diagram in Fig. 1 is an effective vertex with the "local" neutrino integrated out as explained above. This effective coupling takes the form

$$\Delta \mathcal{L} = \frac{1}{2} (\delta h)^2 \mathcal{O}_2, \qquad \mathcal{O}_2 \equiv \frac{1}{\Lambda} (e^{i\varphi_5} \psi_1 \psi_2 + \text{c.c.}), \quad (8)$$

where we denote the absolute value of effective coupling $y_{12}(y_{11}/m_1 + y_{22}/m_2)$ by an effective cutoff $1/\Lambda$ and its phase by φ_5.

We take Wick contraction and the spinor trace to get

$$\langle \mathcal{O}_1(x) \mathcal{O}_2(y) \rangle = -\frac{4y_{12}}{\Lambda} [\cos(\varphi_{12} + \varphi_5) g_{m_1}(x, y) g_{m_2}(x, y)$$
$$+ \cos(\varphi_{12} - \varphi_5) f_{m_1}(x, y) f_{m_2}(x, y)]. \quad (9)$$

Here, g_m and f_m are functions of mass m and positions $x = (\tau_1, X)$ and $y = (\tau_2, 0)$, given explicitly in [31]. The minus sign comes from the anticommutativity of spinors.

The oscillatory signal in CHC bispectrum can be found by expanding f_m and g_m in the late time limit $\tau_{1,2} \to 0$:

$$if_m(x, y) = 2\text{Re}\left\{ \frac{\Gamma(2 - i\tilde{m})\Gamma(\frac{1}{2} + i\tilde{m})}{4\pi^{5/2}} \left(\frac{\tau_1 \tau_2}{X^2}\right)^{3/2 - i\tilde{m}} \right.$$
$$\left. \times \left[1 + \frac{[3 - 4\tilde{m}(2i + \tilde{m})](\tau_1^2 + \tau_2^2) - 6\tau_1\tau_2}{2(1 - 2i\tilde{m})X^2}\right] \right\}, \quad (10)$$

$$g_m(x, y) = 2\text{Re}\left\{ \frac{\Gamma(2 - i\tilde{m})\Gamma(\frac{1}{2} + i\tilde{m})}{4\pi^{5/2}} \left(\frac{\tau_1 \tau_2}{X^2}\right)^{3/2 - i\tilde{m}} \right.$$
$$\left. \times \left[1 + \frac{[3 - 4\tilde{m}(2i + \tilde{m})](\tau_1^2 + \tau_2^2) + 6\tau_1\tau_2}{2(1 - 2i\tilde{m})X^2}\right] \right\}. \quad (11)$$

Here and later, any mass with a tilde denotes its dimensionless value in unit of H, namely $\tilde{m} = m/H$, and $X \equiv |X|$. We see that if_m and g_m are identical at the leading order and differ at subleading orders. This has important consequences. First, for pure Dirac mass, the Yukawa coupling is diagonalizable with real eigenvalues. Therefore, in Eq. (9), $\langle \mathcal{O}_1 \mathcal{O}_2 \rangle$ is proportional to $f_{m_i}^2 + g_{m_i}^2$ ($i = 1, 2$). This combination is zero at the leading order in $\tau \to 0$ limit, and shows up only at subleading orders in τ. In the in-in correlator, the power-law dependence on τ gets translated to a scaling in the k ratio. Consequently, the signal with only Dirac mass decays faster than naively expected in the squeezed limit. This result is known [31,34] and is compatible with the scenario of Dirac neutrino and Dirac leptogenesis. Second, if there is a Majorana-mass-induced mixed Yukawa coupling but without CP phases, the correlator [Eq. (9)] would be proportional to

$f_{m_1} f_{m_2} + g_{m_1} g_{m_2}$ with $m_1 \neq m_2$. Consequently, a piece proportional to $(\tau_1 \tau_2)^{\pm i(\tilde{m}_1 - \tilde{m}_2)}$ is not canceled out at the leading order. We then expect to see an oscillating signal at the leading order of squeezeness with a *single* frequency given by $\tilde{m}_1 - \tilde{m}_2$. The other combination $\tilde{m}_1 + \tilde{m}_2$ gets canceled for the same reason as the Dirac case. Third, if, in addition, the mixed Yukawa coupling contains irremovable *CP* phases (as in the realistic leptogenesis models), the signal would be proportional to $\cos(\varphi_{12} + \varphi_5) f_{m_1} f_{m_2} + \cos(\varphi_{12} - \varphi_5) g_{m_1} g_{m_2}$. Then, both $(\tau_1 \tau_2)^{\pm i(\tilde{m}_1 - \tilde{m}_2)}$ and $(\tau_1 \tau_2)^{\pm i(\tilde{m}_1 + \tilde{m}_2)}$ show up at the leading order for generic φ_{12} and φ_5. Therefore, this new feature would reveal itself as two distinct sets of oscillation modes in the CHC signature at the leading order of the squeezeness.

It is straightforward to compute the three-point correlator of δh and the shape function in Eq. (2). The result for non-Dirac case is (see Refs. [31,34] for results of pure Dirac mass)

$$
\lim_{\varrho \to 0} \mathcal{S}(\varrho) = 2R_h^3 P_\zeta^{-1/2} \frac{y_{12}}{\Lambda}
$$
$$
\times \{ \cos\varphi_5 \cos\varphi_{12} \mathrm{Re}[\mathcal{C}(\tilde{m}_1, \tilde{m}_2)\varrho^{2+i(\tilde{m}_1 - \tilde{m}_2)}]
$$
$$
+ \sin\varphi_5 \sin\varphi_{12} \mathrm{Re}[\mathcal{C}(\tilde{m}_1, -\tilde{m}_2)\varrho^{2+i(\tilde{m}_1 + \tilde{m}_2)}] \},
$$
(12)

where

$$
\mathcal{C}(\tilde{m}_1, \tilde{m}_2) = \frac{i}{2^{1+i\tilde{m}_{12}} \pi^5} \frac{1}{\tilde{m}_{12}^2} \left(1 + \frac{i\tilde{m}_{12}}{4}\right)(1 - \cosh \tilde{m}_{12}\pi)
$$
$$
\times \sinh(\tilde{m}_{12}\pi)\Gamma\left(\frac{1}{2} - i\tilde{m}_1\right)\Gamma\left(\frac{1}{2} + i\tilde{m}_2\right)
$$
$$
\times \Gamma(2 + i\tilde{m}_1)\Gamma(2 - i\tilde{m}_2)\Gamma^2(2 + i\tilde{m}_{12})
$$
$$
\times \Gamma(-4 - 2i\tilde{m}_{12}),
$$
(13)

with $\tilde{m}_{12} \equiv \tilde{m}_1 - \tilde{m}_2$. The phase $\mathrm{Arg}\,\mathcal{C}(\tilde{m}_1, \tilde{m}_2)$ gives rise to the phase of the oscillatory signal, namely ϑ in Eq. (2), which can be used to distinguish our signal from other oscillatory loop signals [59].

Figure 2 illustrates the signal shape function for the three cases outlines above, with "Dirac" known in the literature, and "Majorana" and "Majorana + *CP* phases" our new results featuring different oscillation patterns. "Majorana + *CP* phases" is most relevant to a realistic leptogenesis model. The "Majorana" case is also worth noting as it represents a class of models with mass-mixing couplings with new oscillation pattern. We only present results for one pair of mixed mass eigenstates. With three generations of neutrinos, more than one pair of mass eigenstates could contribute to the signal. However, according to Eq. (13), the signal strength depends sensitively on the masses. Thus, in general, we expect only one pair of states to contribute predominantly.
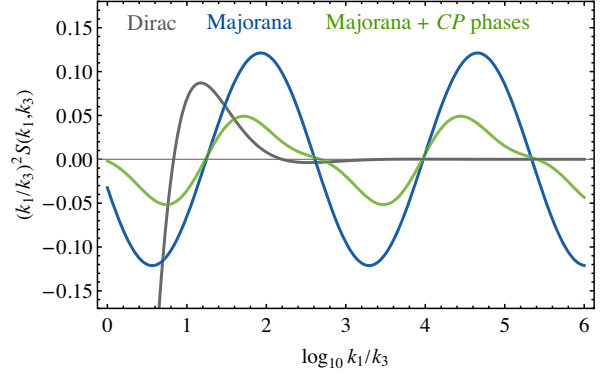

FIG. 2. The oscillatory shape function of the primordial bispectrum [Eq. (12)] as a function of k_1/k_3 for the three cases we consider in the text. We take $m_D = 0.5\,H$ for "Dirac," and take $m_1 = 0.5\,H$ and $m_2 = 1.5\,H$ for both "Majorana" and "Majorana + *CP*." We take $\varphi_{12} = \pi/4$ and $\varphi_5 = -\pi/3$ for "Majorana + *CP*." For all cases we take $R_h^3 y_{12} H/\Lambda = 1$.

In the Supplemental Material [58] we explain details about the Higgs Yukawa couplings with three generations of Majorana neutrinos and present the full calculation for the 3-point correlator of the Higgs fluctuations for the leptogenesis model we consider.

Conditions for baryon asymmetry and results.—We numerically scan parameter space to identify the regions with observable CHC signals and successful leptogenesis. As we can see from Eq. (12), detectable CHC signals favor large Yukawa couplings. But large Yukawa couplings pose a potential tension with leptogenesis as they generally lead to strong washout, which we briefly review now.

The baryon asymmetry Y_B as predicted from leptogenesis can be generally expressed as

$$
Y_B = \frac{c_s}{c_s - 1} \kappa \frac{\epsilon_1}{g_*},
$$
(14)

where $c_s = (8N_f + 4)/(22N_f + 13)$ is the sphaleron conversion efficiency factor, and $c_s = 28/79 \simeq 0.35$ for $N_f = 3$. g_* is the number of relativistic degrees during leptogenesis epoch, which is 106.75 for SM. ϵ_1 is the asymmetry from the decay of heavy RH neutrinos (assuming the lightest N_1 dominates the contribution), given by [60]

$$
\epsilon_1 \simeq -\frac{3}{8\pi} \frac{1}{(y_\nu y_\nu^\dagger)_{11}} \sum_{i=2,3} \mathrm{Im}[(y_\nu y_\nu^\dagger)_{1i}^2] \frac{m_1}{m_i}.
$$
(15)

The above baryon asymmetry is subject to potential reduction by "washout" processes, including the inverse decay and $2 \to 2$ $\not{L}$ scattering, characterized by the washout factor κ, which is the ratio of the decay rate of the RH neutrino, Γ_1, to the Hubble scale H when the temperature equals m_1, $r = \Gamma_1/H(T = m_1)$, i.e.,
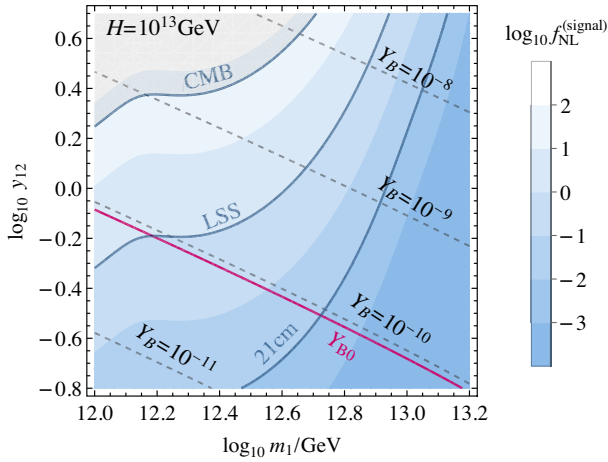
FIG. 3. Contour plots for the amplitude of neutrino signal at CHC $f_{\rm NL}^{\rm (signal)}$ and baryon density Y_B predicted by the leptogenesis model on the 2D plane of Yukawa coupling y_{12} and Majorana RH neutrino mass m_1. The solid red line indicates the observed value of baryon asymmetry, Y_{B0}. The solid blue lines represent experimental sensitivities to $f_{\rm NL}$.

$$r = \frac{M_{\rm Pl}}{32\pi \times 1.7\sqrt{g_*}} \frac{(y_\nu y_\nu^\dagger)_{11}}{m_1}. \qquad (16)$$

$r \ll 1$ is the weak washout regime, while $r \gg 1$ leads to strong washout that significantly suppresses the yield of Y_B. The relation between r and κ can be obtained by solving Boltzmann equations relevant for Y_B evolution [61,62]. For parameters in Fig. 3 we are always in the moderate washout scenario $(10 < r < 10^6)$ where the approximation $\kappa \simeq 0.3/(r \log r)^{0.6}$ works well [62].

In Fig. 3 we show the signal size in Eq. (12) with $m_2 = 2m_1$, and scan over a range of mass m_1 and Yukawa coupling y_{12} within the perturbative regime. More concretely, we take $R_h^3 = 1/2$, $1/\Lambda = y_{12}^2/m_1$, $\varphi_{12} = \pi/4$, $\varphi_5 = -\pi/3$. We also show the predicted baryon asymmetry Y_B with its observed value today $Y_{B0} \equiv [(n_B - n_{\bar{B}})/s] \simeq 8.7 \times 10^{-11}$ from cosmic microwave background and big bang nucleosynthesis related measurements [63,64]. In Fig. 3, leptogenesis parameters realizing the observed value are shown with the solid magenta line, while contours with larger or smaller Y_B are also shown to account for possible late-time dilution or the presence of other sources for baryogenesis.

In Fig. 3 we also include the reach of current cosmic microwave background and forecast for future 21-cm large scale structure observations [40]. As we can see, a good range of the parameter space for viable leptogenesis leads to signals within reach of future cosmic microwave background and 21-cm large scale structure line experiments [65–68]. Furthermore, with a CHC calibrated with known SM processes [34], it is possible to identify the neutrino signals out of SM "backgrounds." The prospect for CHC signals is most distinct and promising when $m_1 \sim H$: for

$m_1 \gg H$, the signal would be strongly suppressed as shown in Fig. 2, while for $m_1 \ll H$ the Majorana mass becomes subdominant to the Dirac mass term—in this case a CHC signal can be observable but restores known patterns in the literature. Furthermore, since the signal strength depends on H mainly through the ratio m_1/H, for a fixed m_1, increasing (decreasing) H in Fig. 3 amounts to shifting all shadings horizontally toward the right (left) side, while the lines remain the same.

Discussion and conclusion.—In this Letter, we propose a new cosmological probe of the well-motivated leptogenesis with Majorana neutrinos, which to date is considered challenging to test directly due to the high energies involved. Specifically, we consider the scenario with SM Higgs contributing to the primordial fluctuation during inflation. Based on cosmological (Higgs) collider physics, we demonstrated that this scenario can lead to observable and distinct imprints of the Higgs' Yukawa couplings to heavy RH Majorana neutrinos and SM neutrinos in the primordial bispectrum. Essential information about leptogenesis, such as the L-violation, heavy RH neutrino masses (in the unit of the inflationary Hubble scale), and the CP phases, can be extracted from delicate measurements of the primordial non-Gaussianity. With a distinct oscillatory feature, our signal is easily distinguishable from the local-shaped NG produced by the Higgs self-coupling [69]. Also, by using the phase information [59], we can further select our signal out of other possible oscillatory signals contributed from addition heavy states, and thus establish the uniqueness of our signal. Our Letter presents an intriguing case of how CC physics may shed light on the profound puzzle of matter-antimatter asymmetry in our Universe, in light of the rich incoming data from cosmic microwave background and large scale structure observations targeting primordial non-Gaussianity.

*Corresponding author.
yanou.cui@ucr.edu
†Corresponding author.
zxianyu@tsinghua.edu.cn

[1] M. Fukugita and T. Yanagida, Phys. Lett. B **174**, 45 (1986).
[2] M. A. Luty, Phys. Rev. D **45**, 455 (1992).
[3] W. Buchmuller, P. Di Bari, and M. Plumacher, Ann. Phys. (Amsterdam) **315**, 305 (2005).

[4] S. Davidson, E. Nardi, and Y. Nir, Phys. Rep. **466**, 105 (2008).

[5] D. Bodeker and W. Buchmuller, Rev. Mod. Phys. **93**, 035004 (2021).

[6] Z.-z. Xing and Z.-h. Zhao, Rep. Prog. Phys. **84**, 066201 (2021).

[7] A. G. Cohen, D. B. Kaplan, and A. E. Nelson, Nucl. Phys. **B349**, 727 (1991).

[8] V. Cirigliano, S. Profumo, and M. J. Ramsey-Musolf, J. High Energy Phys. 07 (2006) 002.

[9] D. E. Morrissey and M. J. Ramsey-Musolf, New J. Phys. **14**, 125003 (2012).

[10] Y. Cui, L. Randall, and B. Shuve, J. High Energy Phys. 04 (2012) 075.

[11] Y. Cui and R. Sundrum, Phys. Rev. D **87**, 116013 (2013).

[12] Y. Cui and B. Shuve, J. High Energy Phys. 02 (2015) 049.

[13] A. E. Nelson and H. Xiao, Phys. Rev. D **100**, 075002 (2019).

[14] Y. Cui and M. Shamma, J. High Energy Phys. 12 (2020) 046.

[15] A. Beniwal, M. Lewicki, J. D. Wells, M. White, and A. G. Williams, J. High Energy Phys. 08 (2017) 108.

[16] M. Chala, G. Nardini, and I. Sobolev, Phys. Rev. D **94**, 055006 (2016).

[17] Y. Cui, Mod. Phys. Lett. A **30**, 1530028 (2015).

[18] Y. Cui, T. Okui, and A. Yunesi, Phys. Rev. D **94**, 115022 (2016).

[19] D. Croon, J. N. Howard, S. Ipek, and T. M. P. Tait, Phys. Rev. D **101**, 055042 (2020).

[20] R. T. Co and K. Harigaya, Phys. Rev. Lett. **124**, 111602 (2020).

[21] G. Elor and R. McGehee, Phys. Rev. D **103**, 035005 (2021).

[22] S. Davidson and A. Ibarra, Phys. Lett. B **535**, 25 (2002).

[23] N. Arkani-Hamed and J. Maldacena, arXiv:1503.08043.

[24] X. Chen, Y. Wang, and Z.-Z. Xianyu, J. High Energy Phys. 08 (2016) 051.

[25] H. Lee, D. Baumann, and G. L. Pimentel, J. High Energy Phys. 12 (2016) 040.

[26] X. Chen, Y. Wang, and Z.-Z. Xianyu, Phys. Rev. Lett. **118**, 261302 (2017).

[27] X. Chen, Y. Wang, and Z.-Z. Xianyu, J. High Energy Phys. 04 (2017) 058.

[28] H. An, M. McAneny, A. K. Ridgway, and M. B. Wise, J. High Energy Phys. 06 (2018) 105.

[29] S. Kumar and R. Sundrum, J. High Energy Phys. 05 (2018) 011.

[30] X. Chen, Y. Wang, and Z.-Z. Xianyu, J. Cosmol. Astropart. Phys. 12 (2017) 006.

[31] X. Chen, Y. Wang, and Z.-Z. Xianyu, J. High Energy Phys. 09 (2018) 022.

[32] Y.-P. Wu, J. High Energy Phys. 04 (2019) 125.

[33] L. Li, T. Nakama, C. M. Sou, Y. Wang, and S. Zhou, J. High Energy Phys. 07 (2019) 067.

[34] S. Lu, Y. Wang, and Z.-Z. Xianyu, J. High Energy Phys. 02 (2020) 011.

[35] T. Liu, X. Tong, Y. Wang, and Z.-Z. Xianyu, J. High Energy Phys. 04 (2020) 189.

[36] A. Hook, J. Huang, and D. Racco, J. High Energy Phys. 01 (2020) 105.

[37] A. Hook, J. Huang, and D. Racco, Phys. Rev. D **101**, 023519 (2020).

[38] S. Kumar and R. Sundrum, J. High Energy Phys. 04 (2020) 077.

[39] S. Alexander, S. J. Gates, L. Jenks, K. Koutrolikos, and E. McDonough, J. High Energy Phys. 10 (2019) 156.

[40] L.-T. Wang and Z.-Z. Xianyu, J. High Energy Phys. 02 (2020) 044.

[41] D.-G. Wang, J. Cosmol. Astropart. Phys. 01 (2020) 046.

[42] Y. Wang and Y. Zhu, J. Cosmol. Astropart. Phys. 04 (2020) 049.

[43] L. Li, S. Lu, Y. Wang, and S. Zhou, J. High Energy Phys. 07 (2020) 231.

[44] L.-T. Wang and Z.-Z. Xianyu, J. High Energy Phys. 11 (2020) 082.

[45] J. Fan and Z.-Z. Xianyu, J. High Energy Phys. 01 (2021) 021.

[46] S. Aoki and M. Yamaguchi, J. High Energy Phys. 04 (2021) 127.

[47] A. Bodas, S. Kumar, and R. Sundrum, J. High Energy Phys. 02 (2021) 079.

[48] N. Maru and A. Okawa, arXiv:2101.10634.

[49] Q. Lu, M. Reece, and Z.-Z. Xianyu, J. High Energy Phys. 12 (2021) 098.

[50] L.-T. Wang, Z.-Z. Xianyu, and Y.-M. Zhong, J. High Energy Phys. 02 (2022) 085.

[51] J. H. Kim, S. Kumar, A. Martin, and Y. Tsai, J. High Energy Phys. 11 (2021) 158.

[52] G. Dvali, A. Gruzinov, and M. Zaldarriaga, Phys. Rev. D **69**, 023505 (2004).

[53] L. Kofman, arXiv:astro-ph/0303614.

[54] T. Suyama and M. Yamaguchi, Phys. Rev. D **77**, 023505 (2008).

[55] K. Ichikawa, T. Suyama, T. Takahashi, and M. Yamaguchi, Phys. Rev. D **78**, 063545 (2008).

[56] A. D. Sakharov, Pis'ma Zh. Eksp. Teor. Fiz. **5**, 32 (1967).

[57] X. Tong, Y. Wang, and Y. Zhu, J. High Energy Phys. 03 (2022) 181.

[58] See Supplemental Material at http://link.aps.org/supplemental/10.1103/PhysRevLett.129.111301 for details about the Higgs Yukawa couplings with three generations of Majorana neutrinos and the full calculation for the 3-point correlator of the Higgs fluctuations for the leptogenesis model we consider.

[59] Z. Qin and Z.-Z. Xianyu, arXiv:2205.01692.

[60] M.-C. Chen, in *Theoretical Advanced Study Institute in Elementary Particle Physics: Exploring New Frontiers Using Colliders and Neutrinos* (2007), pp. 123–176, arXiv:hep-ph/0703087.

[61] E. W. Kolb and S. Wolfram, Phys. Lett. **91B**, 217 (1980).

[62] E. W. Kolb and M. S. Turner, Front.Phys. **69**, 1 (1990).

[63] N. Aghanim *et al.* (Planck Collaboration), Astron. Astrophys. **641**, A6 (2020); **652**, C4(E) (2021).

[64] M. Tanabashi *et al.* (Particle Data Group), Phys. Rev. D **98**, 030001 (2018).

[65] P. D. Meerburg, M. Münchmeyer, J. B. Muñoz, and X. Chen, J. Cosmol. Astropart. Phys. 03 (2017) 050.

[66] A. Moradinezhad Dizgah, H. Lee, J. B. Muñoz, and C. Dvorkin, J. Cosmol. Astropart. Phys. 05 (2018) 013.

[67] P. D. Meerburg *et al.*, arXiv:1903.04409.

[68] K. Kogai, K. Akitsu, F. Schmidt, and Y. Urakawa, J. Cosmol. Astropart. Phys. 03 (2021) 060.

[69] A. De Simone, H. Perrier, and A. Riotto, J. Cosmol. Astropart. Phys. 01 (2013) 037.